LAWRENCE
LIVERMORE
NATIONAL
LABORATORY

LLNL-TR-405968

Virus and Bacterial Cell Chemical Analysis by NanoSIMS

P.K. Weber, J. Holt

August 4, 2008

Disclaimer

This work performed under the auspices of the U.S. Department of Energy by Lawrence Livermore National Laboratory under Contract DE-AC52-07NA27344.

DHS National Laboratory R&D Program Report:

Virus and Bacterial Cell Chemical Analysis by NanoSIMS

Peter K. Weber and Jason Holt
Lawrence Livermore National Laboratory

Thrust Area: Forensics and Attribution, Chemical and Physical Analysis

Date Submitted**:** July 31, 2008

Table of Contents

LLNL-TR-405968

Executive Summary

In past work for the Department of Homeland Security, the LLNL NanoSIMS team has succeeded in extracting quantitative elemental composition at sub-micron resolution from bacterial spores using nanometer-scale secondary ion mass spectrometry (NanoSIMS). The purpose of this task is to test our NanoSIMS capabilities on viruses and bacterial cells. This initial work has proven successful. We imaged Tobacco Mosaic Virus (TMV) and *Bacillus anthracis* Sterne cells using scanning electron microscopy (SEM) and then analyzed those samples by NanoSIMS.

We were able resolve individual viral particles (~18 nm by 300 nm) in the SEM and extract correlated elemental composition in the NanoSIMS. The phosphorous/carbon ratio observed in TMV is comparable to that seen in bacterial spores (0.033), as was the chlorine/carbon ratio (0.11). TMV elemental composition is consistent from spot to spot, and TMV is readily distinguished from debris by NanoSIMS analysis.

Bacterial cells were readily identified in the SEM and relocated in the NanoSIMS for elemental analysis. The *Ba* Sterne cells were observed to have a measurably lower phosphorous/carbon ratio (0.005), as compared to the spores produced in the same run (0.02). The chlorine/carbon ratio was approximately 2.5X larger in the cells (0.2) versus the spores (0.08), while the fluorine/carbon ratio was approximately 10X lower in the cells (0.008) than the spores (0.08). Silicon/carbon ratios for both cells and spores encompassed a comparable range.

The initial data in this study suggest that high resolution analysis is useful because it allows the target agent to be analyzed separate from particulates and other debris. High resolution analysis would also be useful for trace sample analysis.

The next step in this work is to determine the potential utility of elemental signatures in these kinds of samples. We recommend bulk analyses of media and agent samples to determine the range of media compositions in use, and to determine how agent composition relates to media composition. After these baseline analyses are performed, the data should be assessed to determine the potential forensic utility of elemental analyses. If promising, validation studies using bulk or NanoSIMS analysis would be necessary.

Background

As part of the DHS National Laboratory Bioforensics Program, the LLNL NanoSIMS group is developing high resolution, quantitative elemental NanoSIMS analysis methods for forensic applications. NanoSIMS is a high spatial resolution, high sensitivity secondary ion mass spectrometer. Spatial resolution is as good as 50 nm and trace element analysis can be performed at the sub-micron scale.

This capability has been applied to bacterial spores by the LLNL NanoSIMS group (Weber & Ghosal 2006; Weber*, et al.* 2007; Ghosal et al., 2008). Bacterial spores are well suited to high resolution elemental analysis because they are significantly dehydrated relative to vegetative cells[*], they have a symmetric and well-defined internal structure, and they have high mineral content (~4% Ca by weight). Given these characteristics, NanoSIMS can resolve the substructure of individual bacterial spores, and we have demonstrated that individual spore preparations can be differentiated based on NanoSIMS analyses. These results strongly suggest that NanoSIMS can extract forensic information from bacterial spore samples. We are currently undertaking a study to determine the statistical certainty with which bacterial spore samples can be matched using this methodology.

Here we are testing the application of NanoSIMS analysis to virus and bacterial cell samples. In the event of an incident involving such agents, elemental analysis of these kinds of samples could potentially yield forensic information. These samples, however, are potentially more challenging to analyze than bacterial spores. Viral samples are particularly technically challenging because of their size (10s to 100s of nm), and dehydration in the NanoSIMS high vacuum could significantly degrade both viral and vegetative cell samples.

For the virus sample, we chose to analyze tobacco mosaic virus (TMV), a rod-shaped virus that is 300 nm long and 18 nm wide, with a central opening along its axis of 4 nm diameter. TMV consists of single stranded RNA that is helically coiled, with 2130 identical protein subunits, with each subunit covering three nucleotides of the RNA. The precise dimensions and large aspect ratio of this viral particle make it an ideal candidate for evaluating the limits of our electron microscopy and NanoSIMS imaging capabilities.

For the vegetative cell sample, we chose to analyze vegetative cells from an incompletely sporulated *Bacillus anthracis* Sterne sample (NB+Si-W) prepared with elevated dissolved silicon levels. This sample provides the opportunity to compare results from the analysis of spores and vegetative cells from the same sample.

[*] Samples must be dehydrated because NanoSIMS is a high vacuum method.

Methods

Samples

Tobacco mosaic virus samples were obtained from an LLNL source. To prepare these samples, tobacco plants (N. tabacum, L. var. Xanthi) were inoculated by abrading leaves with a stock solution of TMV (5 mg/mL) in 100 mM potassium phosphate buffer, pH = 7.4, containing 1% (w/v) celite. Plant tissue was harvested after the symptoms of virus infection appeared, typically within three to four weeks. Infected leaves were ground with 100 mM potassium phosphate, pH = 7.4, containing 0.1% (v/v) β-mercaptoethanol using a Waring blender. The sap was filtered through cheesecloth to remove solid debris, and n-butanol was added to a concentration of 8% (v/v). After stirring at 4°C, the sap was further clarified by centrifugation for 10 min at 8000 rpm in a Sorvall GS3 rotor. The virus was precipitated by the addition of sodium chloride (4% w/v) and poly(ethylene glycol) (average MW = 6000, 4% w/v), and the crude virus was pelleted by centrifugation for 10 min at 8000 rpm. The white precipitate was suspended in 10 mM potassium phosphate, pH = 7.0, containing 1% (v/v) Triton X-100, and the solution was layered onto an 8 mL sucrose pad (250 mg/mL) containing 1% Triton X-100 in a 70-mL polycarbonate ultracentrifuge tube. The capsids were isolated by sedimentation through the sucrose pad upon centrifugation at 40,000 rpm for 1 hour in a Beckman Ti-45 rotor. The glassy virus pellet was resuspended overnight at 4°C in 10 mM potassium phosphate, pH = 7.0. The solution was cleared of insoluble debris via low-speed centrifugation, and the sedimentation procedure was repeated. The purified pellet was suspended overnight at 4°C in 10 mM potassium phosphate, pH = 6.8. Finally, the virus solution was homogenized using a Dounce homogenizer and insoluble material was removed by brief low-speed centrifugation. The TMV solution was quantified by measuring absorbance at 260 nm, using an extinction coefficient of 3.0 for a 1 mg/mL solution of purified capsids. Stock solutions of TMV capsids, typically 20-30 mg/mL, were flash frozen in small volumes and stored at -80°C.

TMV samples were prepared for analysis by first vortexing the TMV solution to homogenize the suspension, depositing 10 µL quantities on a gold foil, allowing the droplet to air dry, and subsequently rinsing the surface with deionized water to remove precipitated salts (buffer). The sample was then allowed to air dry for at least 2 hours before imaging.

The *Bacillus anthracis* Sterne vegetative cells were produced at LLNL as part of spore production experiment. The sample was produced using nutrient broth in a shake flask with added SiO_2 (NB+Si-W). Incomplete sporulation resulted in a significant abundance of vegetative cells. The cells and spores together were washed in water three times and deposited on gold foil and air dried for analysis.

Analysis

Samples were imaged in a JEOL 7401F field-emission scanning electron microscope. This instrument incorporates a “gentle beam” mode to facilitate imaging of non-conductive

materials, in particular biological particles such as cells and viruses. Depending on the particular accelerating voltage and imaging mode used, resolutions of between 1.0-1.5 nm can be routinely achieved, making this instrument ideally suited for imaging of sub-cellular structures and viral particles.

NanoSIMS analysis was performed with a Cameca NanoSIMS 50 at LLNL. A focused Cs^+ primary beam was stepped over the samples to generate serial element specific digital images (typically 256 x 256 pixels). Higher resolution was used for the virus sample (50 nm, 0.3 pA versus ~100 nm, 2 pA). Viral particles were analzyed for $^{12}C^-$, $^{12}C^{14}N^-$, $^{31}P^-$, $^{32}S^-$, and $^{35}Cl^-$ with simultaneous detection. Bacterial cells were analzyed for $^{12}C^-$, $^{19}F^-$, $^{28}Si^-$, $^{31}P^-$, and $^{35}Cl^-$. The data images were processed using L'Image (L. Nittler, Carnegie Institute of Washington) to generate regions-specific depth profiles and depth-averaged elemental ratios for quantification.

Results and Discussion

Virus

A tobacco mosaic virus (TMV) sample was analyzed by SEM and NanoSIMS, as shown in Figure 1. The TMV sample presents particular challenges with respect to imaging and NanoSIMS analysis, given its morphology. TMV is a rod-shaped virus that is 0.3 μm long and 18 nm in diameter. Using the high resolution capability of the JEOL 7401 SEM, however, we were able to identify individual virus particles and perform a subsequent NanoSIMS depth profile analysis. Table 1 lists the elemental compositions in regions highlighted in Figure 1. The phosphorous/carbon ratio observed with this sample is comparable to that seen in bacterial spores (0.03), arising in this case from the RNA material encapsulated within the viral particle, as opposed to the DNA, RNA and ADP located in the spore core region. The sulfur content is similar to what is found in spores and other biological material (S/C ~ 0.1 or [S] ~1%).

Despite possessing orders of magnitude less material than a spore (~0.1 fg versus 1 pg), viral particles can be analyzed and distinguished from non-viral material present in a given sample (Table 1). Material that does not have the TMV morphology (region 5) has anomalously high (~10x) phosphorous/carbon ratio (0.43), sulfur/carbon (2.3) and chlorine/carbon (0.81) ratios. This significant difference in composition further confirms that this material is non-viral.

It is also notable that the elemental composition of the TMV particles is as homogenous as the most homogenous elements in bacterial spores (e.g., P, N and S). This is particularly notable for Cl, which in bacterial spores can have 100% relative standard deviation (RSD). Low variability in these measurements is another indication that there is sufficient material in the TMV particles to make accurate and precise measurements.

Sample preparation and pre-NanoSIMS high resolution SEM imaging are critical to the success of these analyses. Here, the sample was sufficiently dispersed to enable

individual viral particles and aggregated viral particles to be identified in the SEM and analyzed in the NanoSIMS. This work would be significantly more challenging for viral samples that cannot be clearly identified based on morphology. However, it should be noted that in cases where high resolution SEM can not differentiate viral particles from debris, atomic force microscopy (AFM) could be used for sample imaging and viral particle identification (Malkin*, et al.* 2003; Malkin*, et al.* 2005; Malkin*, et al.* 2008). We have performed correlated AFM and NanoSIMS analysis for previous work with Alex Malkin at LLNL.

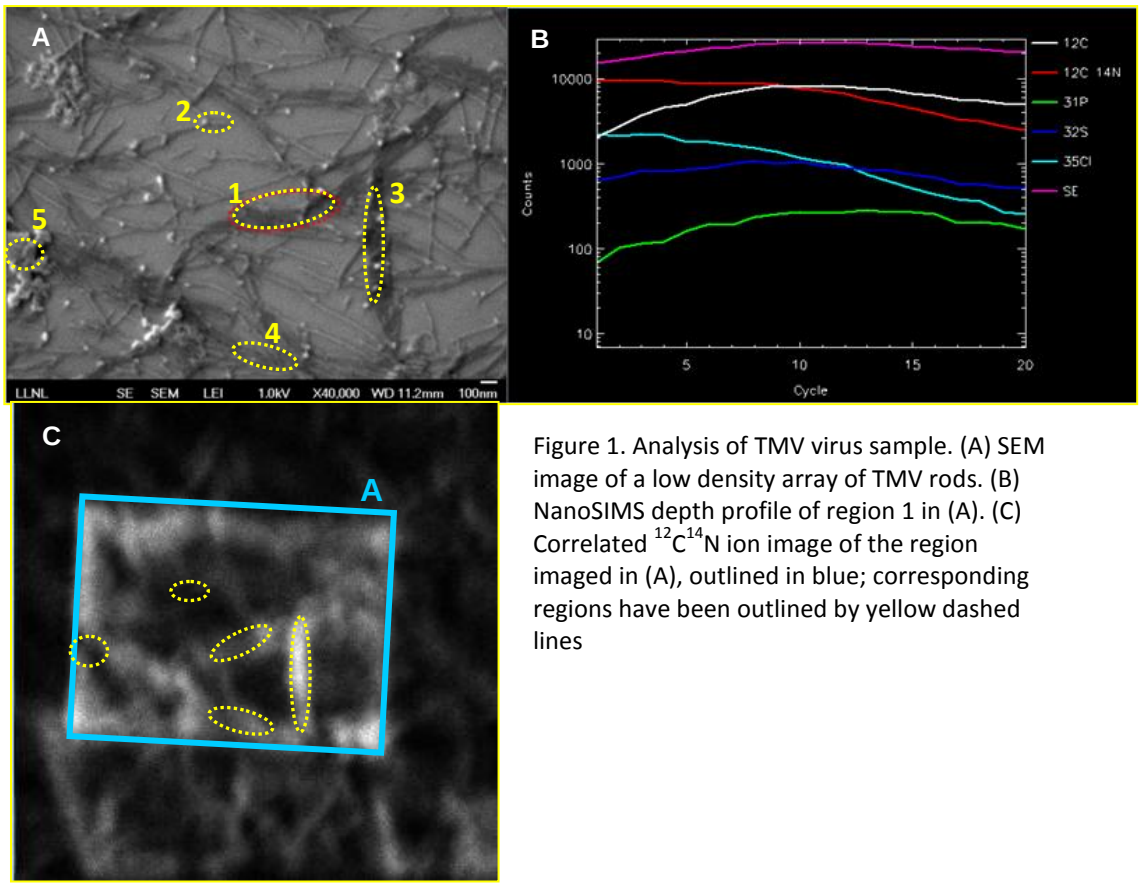

Figure 1. Analysis of TMV virus sample. (A) SEM image of a low density array of TMV rods. (B) NanoSIMS depth profile of region 1 in (A). (C) Correlated $^{12}C^{14}N$ ion image of the region imaged in (A), outlined in blue; corresponding regions have been outlined by yellow dashed lines

Table 1. Elemental distributions within selected regions of TMV sample.

Region	*Material*	*$^{12}C^{14}N/^{12}C$*	*$^{31}P/^{12}C$*	*$^{32}S/^{12}C$*	*$^{35}Cl/^{12}C$*
1	viral	0.78	0.032	0.11	0.11
2	viral	0.70	0.029	0.16	0.13
3	viral	0.83	0.037	0.13	0.11
4	viral	0.71	0.032	0.096	0.080
5	*non-viral*	*1.1*	*0.43*	*2.3*	*0.81*
average	**viral**	**0.75**	**0.032**	**0.12**	**0.11**
SD	**viral**	**0.061**	**0.0033**	**0.028**	**0.021**
RSD	**viral**	**0.08**	**0.10**	**0.22**	**0.19**

Vegetative Cells

Using SEM, vegetative cells were identified in the *B. anthracis* Sterne sample NB+Si-W (Fig. 2). The SEM image shows that the cells are flatter and more diffuse-looking than a spore, requiring high resolution to distinguish them from the background. Imaged cells were mapped to enable correlated NanoSIMS (depth profile) analysis on those specific cells, as indicated in Figure 2. Significant counts of all species were collected, enabling quantification (Table 2). Based on the number of carbon ions collected from the cells, the dry mass of the cells is similar to that of spores.

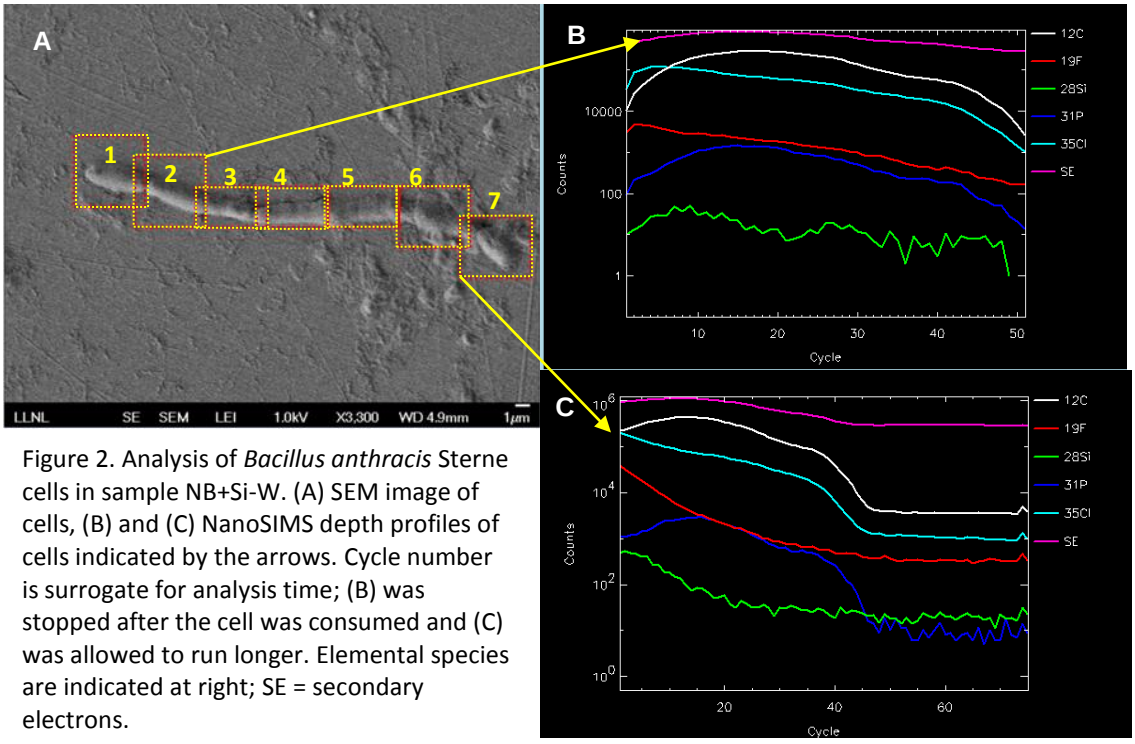

Figure 2. Analysis of *Bacillus anthracis* Sterne cells in sample NB+Si-W. (A) SEM image of cells, (B) and (C) NanoSIMS depth profiles of cells indicated by the arrows. Cycle number is surrogate for analysis time; (B) was stopped after the cell was consumed and (C) was allowed to run longer. Elemental species are indicated at right; SE = secondary electrons.

Table 2. Elemental concentrations of cells indicated in the SEM image of Figure 2(A).

Cell	*F/C*	*Cl/C*	*Si/C*	*P/C*
1	0.012	0.37	1.7E-4	0.006
2	0.006	0.22	8.5E-5	0.005
3	0.006	0.19	6.3E-5	0.005
4	0.015	0.26	1.9E-4	0.005
5	0.005	0.11	1.4E-4	0.004
6	0.005	0.14	1.3E-4	0.006
7	0.004	0.11	1.4E-4	0.007
Average	**0.008**	**0.2**	**1.3E-4**	**0.005**
standard deviation	**0.0042**	**0.094**	**4.5E-05**	**0.00098**
RSD	**0.52**	**0.47**	**0.34**	**0.20**

The elemental composition of the vegetative cells and spores from this sample are compared in Table 3. The phosphorous/carbon ratio in the cells is substantially lower than in the spores (0.005 versus 0.02; Weber & Ghosal 2006; Ghosal*, et al.* 2008;), the same as observed in *Anabaena oscillarioides* (0.005; Popa*, et al.* 2007) and low compared to *Schewanella oneidensis* MR-1 (0.03; P.K. Weber unpublished data). The fluorine content of the cells is also substantially lower than seen in the spores. This result can be explained by the fact that F^- is not an important anion in cells, whereas the spore coat (to some extent, the core) have affinity for F (Weber & Ghosal 2006; Ghosal*, et al.* 2008; Ghosal*, et al.* in submission). On the other hand, the chlorine content of cells is twice and that in spores, presumably because Cl^- is an important anion in cells, but the spore coat also has significant affinity for Cl (Weber & Ghosal 2006; Ghosal*, et al.* 2008; Ghosal*, et al.* in submission). Interestingly, the Si content in the cells is approximately half that of the spores in this sample. In our work studying Si in spores, we found that the affinity of spores for Si is greater than or equal to the reported affinity of *Bacillus* cells for Si (Weber*, et al.* 2008). This result is in agreement with our findings in that study.

Table 3. Comparison of cell and spore elemental composition in sample NB+Si-W.

sample type	*P/C*	*F/C*	*Cl/C*	*Si (μg/g)*
cells	0.005	0.008	0.2	110
spores	0.02	0.08	0.08	257

Future Directions

These experiments demonstrate the viability of virus and cell analysis using combined high resolution morphological analysis with SEM, and high spatial resolution chemical analysis with the NanoSIMS. Further work will be necessary to determine the ultimate forensic utility of virus and vegetative cell elemental analyses. Elemental composition could potentially provide information on the production media, the production method, and/or post-processing of the sample. To determine the utility of linking a virus or vegetative cell sample to the media, it would be useful to determine the range of elemental composition in media used to produce specific samples, and to determine how closely the samples reflect the production media. In the case of bacterial spores, we have shown that differences in media are reflected in the spores. It will also be important to consider post-processing, which has the potential to significantly alter sample elemental composition. While this work has not yet demonstrated that same connection for viruses and vegetative cells, it has demonstrated our capability for high fidelity chemical analyses of viruses and vegetative cells.

Another important question will be, What specific forensic utility is NanoSIMS analysis for these samples? In the case of bacterial spores, quantitative high spatial resolution analysis is particularly useful because (1) it enables spores to be analyzed independently from other material in the sample, (2) it enables differences in the elemental distribution within spores to be identified, and (3) it enables analysis of ultra-trace

samples (<100 spores). For viruses and vegetative cells, the high resolution of the NanoSIMS is likely to useful, at least for insuring the correct material is analyzed and for trace samples. The central question will be, Are there specific elemental or isotopic signatures for these samples that will be of forensic utility? Therefore, we believe that the first steps in this process are the ones identified above.

Acknowledgements

This work was funded by the Department of Homeland Security. Andrew Presley and Sunwook Lee provided the TMV sample. Joanne Horn, Sue Martin and Christina Ramon produced the *Bacillus anthracis* Sterne sample at LLNL. Steve Velsko and Kris Montgomery provided valuable insights. This work was performed under the auspices of the U.S. Department of Energy by Lawrence Livermore National Laboratory under Contract DE-AC52-07NA27344.

References

Ghosal, S., S.J. Fallon, T. Leighton, K.E. Wheeler, I.D. Hutcheon, P.K. Weber (2008) Imaging and 3D elemental characterization of intact bacterial spores with high-resolution secondary ion mass spectrometry (NanoSIMS) depth profile analysis. Analytical Chemistry

Ghosal, S., T. Leighton, K. Wheeler, I.D. Hutcheon, P.K. Weber (in review) Analysis of bacterial spore permeability to water and ions using nano-secondary ion mass spectrometry (NanoSIMS). Environmental Science and Technology.

Malkin, A.J., Y.G. Kuznetsov, M.Plomp, A. McPherson (2008) Virus architecture probed by atomic force microscopy. Structure-based study of viral replication 289-310.

Malkin, A.J., A. McPherson, P.D. Gershon (2003) Structure of intracellular mature vaccinia virus visualized by in situ AFM. Journal of Virology *77*, 6332–6340.

Malkin, A.J., M. Plomp, A. McPherson (2005) Unraveling of the architecture of viruses by high-resolution atomic force microscopy. DNA Viruses: Methods and Protocols 85-108.

Popa, R., P.K. Weber, J. Pett-Ridge, J.A. Finzi, S.J. Fallon, I.D. Hutcheon, K.H. Nealson, D.G. Capone (2007) Carbon and nitrogen fixation and metabolite exchange in and between individual cells of *Anabaena oscillarioides*. The International Society of Microbial Ecology Journal *1*, 354-360.

Weber, P.K., S. Ghosal (2006) Elemental Gradients and Diffusion in Spores. Report to the Department of Homeland Security.

Weber, P.K., S. Ghosal, I.D. Hutcheon, T. J. Leighton, K.E. Wheeler (2007) Silicon and Metal Signatures of Bacteria. Report to the Federal Bureau of Investigation.

Weber, P.K., B. Viani, J. Holt, M.L. Davisson (2008) Si uptake and modeling in Bacillus anthracis spores. Report to the Department of Homeland Security.